Graefe's Arch Clin Exp Ophthalmol (2007) 245:835–846
DOI 10.1007/s00417-006-0437-9

LABORATORY INVESTIGATION

Long-term neuroretinal full-thickness transplants in a large animal model of severe retinitis pigmentosa

Fredrik Ghosh · Karl Engelsberg · Robert V. English · Robert M. Petters

Received: 14 June 2006 / Revised: 23 July 2006 / Accepted: 31 July 2006 / Published online: 27 October 2006

Abstract
Background The purpose of this study was to explore neuroretinal transplantation in a large animal model of severe retinitis pigmentosa and to establish graft development, long-term survival, graft-host integration, and effects on the host retina.
Methods Rhodopsin transgenic pigs, aged 6 months, received in one eye a fetal full-thickness neuroretinal sheet in the subretinal space by means of vitrectomy and retinotomy. Six months postoperatively, eyes were studied in the light microscope and with immunohistochemical markers. Full-field electroretinography (ERG) was performed at 4 and 6 months.
Results Laminated grafts with well-organized photoreceptors, rod bipolar cells, and Müller cells were found in five of six eyes. Neuronal connections between graft and host retina were not seen. In the five eyes containing a graft, the number of surviving rods in the host retina was significantly higher compared with unoperated eyes. The ERG did not reveal any significant difference in b-wave amplitude between operated and control eyes, but the cone-derived response in operated eyes increased significantly from 4 to 6 months while the rod response in control eyes decreased significantly.
Conclusions Fetal full-thickness neuroretina can be transplanted safely to an eye with severe retinal degeneration. In their major part, the transplants develop a normal laminated morphology and survive for at least 6 months. Graft and host retinal neurons do not form connections. Retinal function in the host is reduced initially by the surgical trauma, but the presence of a well-laminated graft counteracts this effect and rescues rods from degeneration.

Keywords Immune privilege · Photoreceptor morphology · Retinal degeneration · Vitreoretinal surgery

Introduction

Retinal transplantation experiments, aimed at alleviating visual impairment caused by degeneration of photoreceptors in retinitis pigmentosa (RP) and age-related macular degeneration, have been ongoing for almost two decades [30]. During this period, much progress has been made but, to date, retinal transplantation is not available as a clinical treatment.

A handful of experimental studies have shown that neuroretinal transplants can survive and maintain morphologically normal photoreceptors for extended time periods if they are placed in their homotopic location in the subretinal space with correct polarity [13, 16, 17, 29, 32]. Progress has also been made in the critical area of neuronal integration between host and graft retinal neurons, but this problem has not yet been adequately solved, making

Supported by The Foundation Fighting Blindness (grant# C-NC02-798-0078), The Faculty of Medicine, University of Lund, The Swedish Research Council, The Princess Margaretas Foundation for Blind Children, The 2nd ONCE International Award for New Technologies for the Blind.

F. Ghosh (✉) · K. Engelsberg
Department of Ophthalmology, BMC, Lund University Hospital, 22184 Lund, Sweden
e-mail: fredrik.ghosh@med.lu.se

R. V. English
College of Veterinary Medicine, North Carolina State University, Raleigh, NC, USA

R. M. Petters
Department of Animal Science, North Carolina State University, Raleigh, NC, USA

transmission of visual information from graft to host improbable [12, 21, 28].

In the strive towards curing patients, models closely resembling human retinal degenerative disease are of great value. One significant advancement in this field is the development of the rhodopsin transgenic pig which is a large animal model featuring a human form of RP [2]. This model, first described in 1997, involves the rhodopsin mutation Pro347Leu, which in the first year of life causes severe loss of rods [25]. We previously reported transplantation of neonatal normal full-thickness neuroretina to young rhodopsin transgenic pigs and found that such grafts survive and develop well for at least 4 months in the diseased eye [16]. However, the study did not show integration between graft and host retinal neurons since the neonatal retina kept its inherent synaptic architecture and did not sprout new neuronal fibers towards the host. Additionally, 1–3 rows of photoreceptors remained in the host retina straddling the graft which hampered fusion.

For the present study, we wanted to expand knowledge gained from our earlier experiment. We chose to study transplantation of fetal instead of neonatal neuroretina to see if the greater plasticity of such tissue would enhance graft-host integration. Another rationale for using fetal donor tissue is that in contrast to neonatal tissue, it is available after ethical approval and has been used for clinical transplantation trials in RP patients as well as in patients suffering from Parkinson's disease [3, 6]. To further promote graft-host integration, we used host eyes more severely affected by the disease, i.e., with a retina in which very few of the rod photoreceptors remain, corresponding to an RP patient with a significant reduction in vision.

We also wanted to explore the hypothesis that rod photoreceptors in a retina severely affected by degenerative disease can still be rescued by the presence of a well-developed neuroretinal graft. Several studies have indicated an improved retinal function after transplantation, which in a few morphological reports has been ascribed to a rescue of host cone photoreceptors [1, 21, 24, 26, 27]. The effect of retinal transplantation on remaining host rod photoreceptors has so far been difficult to assess, since experiments have been limited to small animal models in which rods degenerate very rapidly. The use of a large animal model like the rhodopsin transgenic pig may in this setting be favorable, since rod degeneration is comparably slower than in smaller animals.

The goals of this study thus were:

1. To investigate development and long-time survival of fetal neuroretinal grafts in a large animal model eye of severe RP
2. To examine neuronal and glial interactions of host and graft retina
3. To explore the morphology and function of remaining rod photoreceptors in the host

Methods

Donor tissue

One normal pregnant Yorkshire cross pig was euthanized by means of captive bolt and incision of the carotid arteries. Eight fetuses, aged E48 (48 days post conception), were taken out by cesarean section. At this stage, the major part of the neuroretina consists of an outer neuroblastic layer and a ganglion cell layer with multiple rows of cells (Fig. 1a). The 16 eyes were collected by enucleation, immediately immersed in CO_2-independent medium (Gibco, Paisley, UK), and rinsed from excessive tissue. The anterior segment and vitreous were removed, and the neuroretina carefully dissected out by gently teasing it from the retinal pigment epithelium (RPE) using microforceps and cutting at the optic nerve head. One eyecup was fixed immediately, without dissection of the neuroretina, to be used as control. Six of the neuroretinas were kept in Ames' solution on ice to be used for the first session of transplantations the same day. Nine neuroretinas were put in tissue culture to be used for transplantation the following day (Fig. 1b). These nine neuroretinas were cut into circular pieces, measuring approximately 3–4 mm in diameter, and

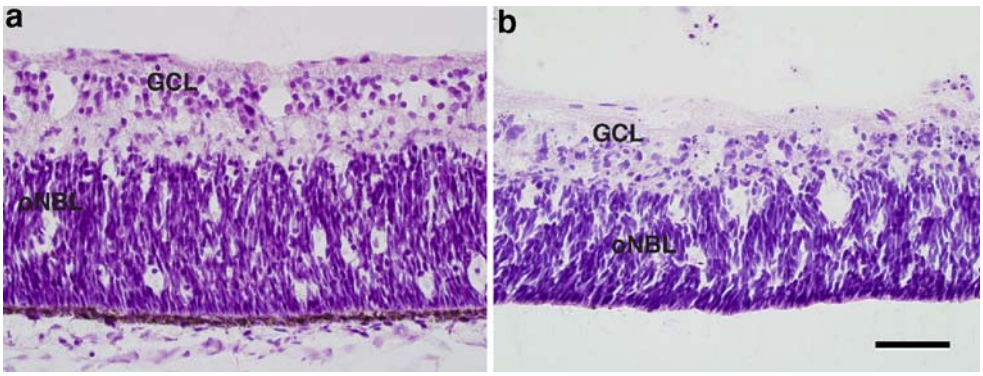

Fig. 1 **a** Hematoxylin and eosin staining of fetal E48 (48 days after conception) retina (central part). The normal retinal layers have not yet developed, and the neuroretina consists of an outer neuroblastic layer (*oNBL*) and ganglion cell layer (*GCL*). **b** Fetal E48 neuroretina kept in vitro for 28 h (central part). The neuroretina has kept its laminated architecture but is thinner than the specimen in **a**. Scale bar=50 μm

were explanted on a Millicell-PCF 0.4 mm culture plate insert (Millipore, Bedford, MA, USA) with the photoreceptor layer facing the membrane. The explants were cultured in Dulbecco's modified Eagle's medium F-12 (DMEM/F12) supplemented with 10% fetal calf serum and maintained at 37°C with 95% humidity and 5% CO_2. A mixture of antibiotics containing 2 mM L-glutamine, 100 U/ml penicillin, and 100 ng/ml streptomycin (Sigma-Aldrich, Gillingham, UK) was added. Just before actual transplantation, rectangular pieces measuring 2×3 mm were cut from one of the neuroretinas. All excess tissue was fixed and processed for histology.

Hosts

Six Pro347Leu rhodopsin transgenic pigs, aged 6 months (181–182 days), were used as hosts. At this stage, the rod photoreceptors have degenerated severely, and the outer nuclear layer (ONL) is reduced from the normal 8 rows of cells to 1–3 rows of cells (Fig. 2a,b) [22].

Surgical procedures

The surgical procedures were, with a few exceptions, identical to the one reported in a previous paper [16], and will only be summarized here. Six consecutive animals were operated in two sessions of three animals each. All operations were documented using a video camera connected to the operating microscope.

The host pig was put under general anesthesia. A two-port core vitrectomy including posterior vitreous detachment was performed, using a vitreous cutter and a combined light and irrigation instrument. A blunt 30G needle, attached to a 1.0-ml syringe filled with Ames' solution through a polyethylene tube, was used to create a 4- to 6-mm area of neuroretinal detachment in the central vessel-free retina by means of a retinotomy. This retinotomy was then enlarged and a second small retinotomy was made in the inferior part of the detachment bleb. The transplant was drawn into a siliconized glass cannula connected to a 1.0-ml syringe via a polyethylene tube. The cannula was introduced into the eye through the 10 o'clock sclerotomy and its end positioned against the superior retinotomy. Finally, the transplant was pushed out of the cannula into the subretinal bleb with the future photoreceptor side oriented towards the host retinal pigment epithelium (Fig. 3). One graft per eye was used. Three eyes received a neuroretina harvested the same day, within 6 h from harvest of the donor eye (pig #1–3), and the remaining three received a neuroretina kept in tissue culture for 24–28 h (pig #4–6). The operation time varied between 30 and 40 min.

Postoperative management

No postoperative treatment was given. The eyes were examined externally daily, and ophthalmoscopically on two occasions, on postoperative days 1–2 and after 4 months.

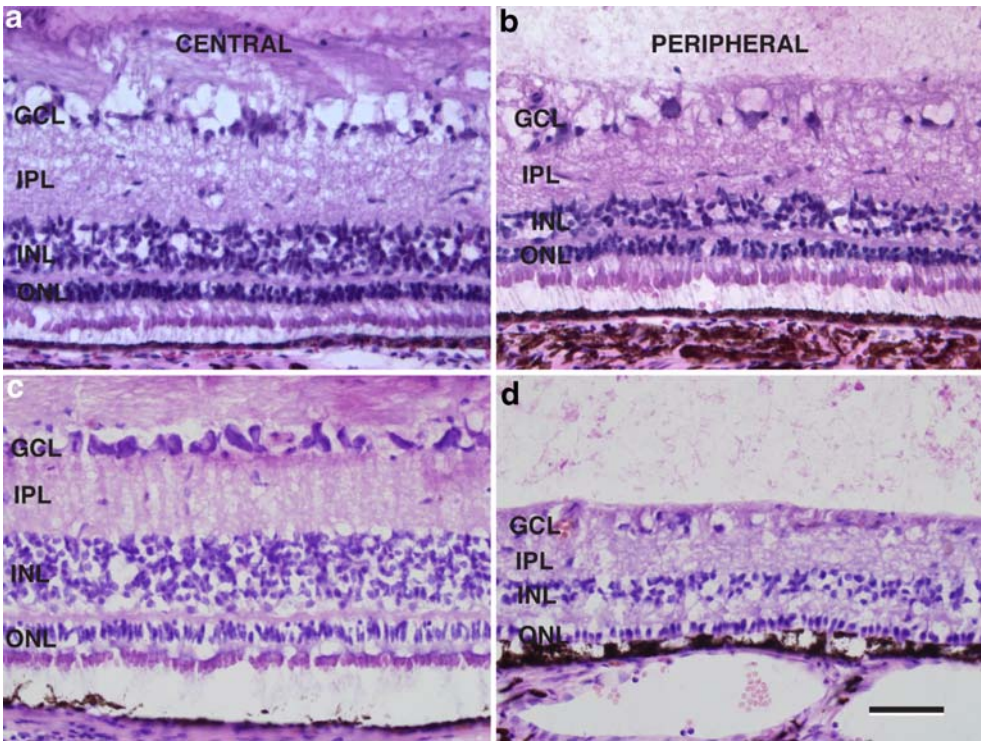

Fig. 2 Hematoxylin and eosin staining of rhodopsin transgenic retina at 6 months (**a** and **b**) and 12 months (**c** and **d**). The outer nuclear layer (*ONL*) is reduced from the normal 8 rows of cells to 1–2 rows. In **a**–**c**, the inner retinal layers (*INL*, *IPL*, *GCL*) are relatively intact, but in the peripheral 12-month retina, all layers are affected. Scale bar=50 μm

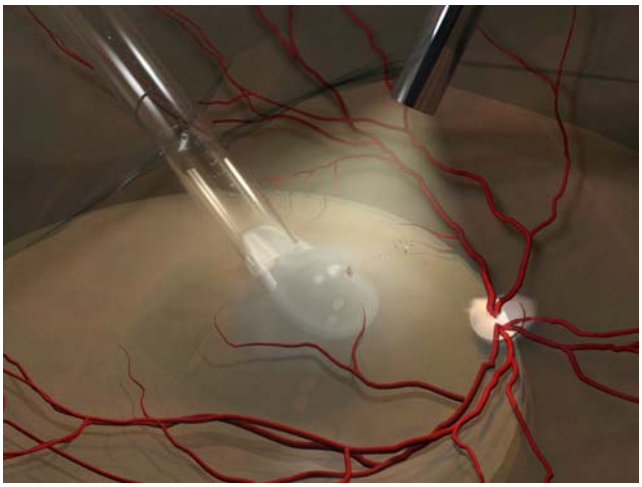

Fig. 3 Illustration of the transplantation procedure. After a core vitrectomy including a posterior vitreous detachment, a local neuroretinal detachment has been created by infusing Ames' solution through a retinotomy and into the subretinal space. A second pinpoint retinotomy is made in the bleb and the first retinotomy is slightly enlarged. The full-thickness transplant, drawn into a siliconized glass capillary, is introduced into the eye and pushed out into the subretinal space using fluid from an attached syringe. As the graft enters the subretinal space, the excess fluid escapes through the second retinotomy

Full-field electroretinography (ERG) was performed on all pigs in both eyes (see below) 4 and 6 months after surgery. The animals were killed 6 months after the transplantation with 80 mg/kg sodium pentobarbital (390 mg/ml) intravenously after sedation with a mixture of 13 mg/kg ketamine HCl (100 mg/ml) and 2 mg/kg xylazine (100 mg/ml) in the neck muscle.

All proceedings and animal treatment were in accordance with the guidelines and requirements of the Government Committee on Animal Experimentation at Lund University and the "Principles of Laboratory Animal Care" (NIH publication No. 85-23, revised 1985), the OPRR Public Health Service Policy on the Humane Care and Use of Laboratory Animals (revised 1986), and the US Animal Welfare Act, as amended, were followed.

ERG

Animals were dark adapted for 90 min and sedated with an intramuscular injection (0.03 ml/kg) of a combination of telazol (20 mg/ml), ketamine (50 mg/ml), and xylazine (50 mg/ml). Tropicamide 1% was administered to both eyes 60 and 30 min prior to electrophysiologic evaluation. Pulse oximetry and respiratory rate were monitored throughout the sedation period.

Using computer-based electrodiagnostic equipment (BPM-100 and Retinographics software, Retinographics, Norwalk, CT, USA), responses were measured under scotopic conditions with an ERG Jet gold contact lens electrode (Nicolet Biomedical #842-216700, Fitchburg, WI, USA) on the cornea and a Grass platinum subdermal electrode (Grass Instruments #E2-48, Braintree, MA, USA) 2 cm from the lateral canthus. A ground platinum electrode was placed between the scapulae. Light stimulus was accomplished using a white light-emitting diode (LED) array. The spectrum of the white LED was centered at 500 nm. Eight increasing levels of flash intensity were used, and three single flashes at each intensity were recorded 60 s apart. The stimulus levels used included low levels near the rod threshold response up to high levels capable of generating robust responses from both rod and cone cells in normal retina. The program assigned the flashes the following dB values: −30, −25, −20, −15, −10, −5, 0, and +5. Specifically, the stimuli levels, in scotopic-candela.seconds.m^{-2}, were −2.8, −2.5, −1.9, −1.3, −0.35, 0.67, 1.0, and 1.7. The person recording the electrophysiologic responses, and the person reading the b-wave amplitude, were blinded to which eye had received surgery. The two lowest stimulus levels (−30 and −25 dB) yielded no detectable responses in any of the transplanted or control eyes, but robust rod responses were obtained at the −20 dB intensity in all eyes, whereas the +5 dB stimulus resulted in a near maximal cone-rod response. For statistical analysis, the mean value of b-wave amplitudes obtained at −20 dB as well as +5 dB from each eye at each time point was used. The Wilcoxon matched pairs signed ranks test was used to compare unoperated with control eyes at each time point, and also the change in response from 4–6 months postoperatively of operated as well as control eyes. Statistical significance was defined as $p<0.05$. GraphPad InStat (GraphPad Software, San Diego, CA, USA) was used for calculations.

Tissue preparation

For light microscopy, both eyes from each animal were enucleated and fixed for 30 min in formaldehyde (4%, generated from paraformaldehyde) at pH 7.3 in a 0.1 M Sørensen's phosphate buffer. The anterior segment was then removed and the posterior eyecup was postfixed in the same solution for 4 h. All eyecups were examined in an operating microscope (Carl Zeiss, Oberkochen, Germany) and photographed using an attached digital camera (Sony, Tokyo, Japan). After fixation, the specimens were washed with Sørensen's phosphate buffer (0.1 M, pH 7.4) and then washed again using the same solution with added sucrose of rising concentrations (5–30%). Tissue specimens were obtained as approximately 4-mm wide pieces, including the optic nerve. In transplanted eyes, the complete graft was included, and the corresponding area was obtained in the unoperated eye. The specimens were serially sectioned at

12 μm on a cryostat and stained with hematoxylin and eosin according to standard procedures.

For immunohistochemistry, sections processed in the manner above were thawed and washed in 0.1 M sodium phosphate-buffered saline (PBS) with 0.25% Triton X-100 (PBS/Triton, pH 7.2) and then incubated overnight with antibodies raised against rhodopsin (for labeling of rod photoreceptors; monoclonal; 1:200; kind gift from Professor S. Molday, University of British Columbia, Vancouver, Canada), transducin-gamma (for labeling of cone photoreceptors; polyclonal; 1:1000; CytoSignal Research Products, UK), protein kinase C [Phospho-PKC (pan); rod bipolar cells; polyclonal; 1:200, Cell Signaling, Beverly, MA, USA], and glial fibrillary acidic protein (GFAP, for labeling of activated Müller cells; monoclonal; 1:1000; Chemicon International, Temecula, CA, USA).

After incubation, the slides were rinsed, incubated with fluorescein isothiocyanate (FITC) or Texas Red (TR)-conjugated antibodies (1:200) for 45 min, rinsed again, and finally mounted in VECTASHIELD mounting medium (Vector Laboratories, Inc., Burlingame, CA, USA). Control experiments on normal adult porcine retina were made with each antibody. For negative controls, the complete labeling procedures without primary antibodies were also performed. Slides were examined using an epifluorescence microscope (Eclipse E800, Nikon, Tokyo, Japan) equipped with a digital acquisition system (DEI-750, Optronics, Goletta, GA, USA).

Quantification and statistical analysis of remaining host rod photoreceptors

Rhodopsin-labeled sections from all unoperated and operated eyes were used for quantification of remaining rods in the host retina. Four sections located at opposite ends of the specimen were evaluated for rhodopsin-labeled cells. Sections were only used if they included two opposite peripheral retinal regions as well as the optic nerve. A graphical representation of each section was drawn on a template containing a scale divided into 50 segments, representing approximately one field of vision using the ×40 objective on the Nikon microscope. Three levels of rhodopsin-labeled cell concentration were used: level 0: scattered cell (drawn white), level 1: 1 continuous row of cells (red-white striped), and level 2: 2 continuous rows of cells (red). Each section was thereafter scored: (total length of level 0×0.25) + (total length of level 1×1) + (total length of level 2×2). Each eye was then scored by obtaining the mean value of the sections. The Wilcoxon matched pairs signed ranks test was used to compare scores from eyes containing transplants with unoperated eyes from each animal. Statistical significance was defined as $p<0.05$. GraphPad InStat (GraphPad Software, San Diego, CA, USA) was used for calculations.

Results

Surgery and macroscopic findings

In all six cases, the full-thickness graft could be placed safely in the subretinal space, and in three eyes, the graft was completely flat at the conclusion of the procedure. Peroperative complications were limited to a minimal lens touch in one eye (pig #1).

The subretinal grafts with a flattened host retinal bleb could be seen in all eyes on the first clinical examination on postoperative days 1–2. One eye displayed a slight vitreal hemorrhage which resolved completely during the following postoperative period (pig #4). The eye in which the lens had been touched during surgery (pig #1) progressively developed a subcapsular cataract and vitreal strands with some traction on the host temporal retina. At 4 months postoperatively, a vitreal membrane extending from the temporal host retina to the posterior lens capsule and a posterior subcapsular cataract was seen in this eye. The remaining five eyes displayed clear media. At dissection, 6 months after the transplantation, all host retinas were found to be attached, in spite of the pulling force of vitreous strands in one eye (pig #1). The graft was identified in the subretinal space in five eyes. In three eyes, the graft was located 3–5 optic disc diameters towards the periphery from the original place of insertion.

Light microscopy

Donor tissue

Specimens kept in culture for 24–28 h displayed a laminated appearance with an outer neuroblastic layer (oNBL) and a ganglion cell layer with multiple rows of cells (Fig. 1b). More enlarged vacuoles were seen within the oNBL and the specimens appeared thinner when compared with the E48 control retina (Fig. 1a).

Graft

Grafts were found in five of the six transplanted eyes. All transplants, in their major part, displayed a laminated appearance with correct polarity and layers parallel to the host RPE (Fig. 4a–d). The length of these grafts ranged from 2.1 to 3.4 mm. All five grafts also displayed a non-laminated part facing the host retina. This part of the graft was in the form of degenerating rosettes or laminated retina with reversed polarity (Fig. 4b–d). The correctly laminated part of the grafts displayed a well-developed outer nuclear layer (ONL) and inner as well as short outer segments. In three of the five grafts, all inner retinal layers had developed (Fig. 4b–d), and in the remaining two, inner

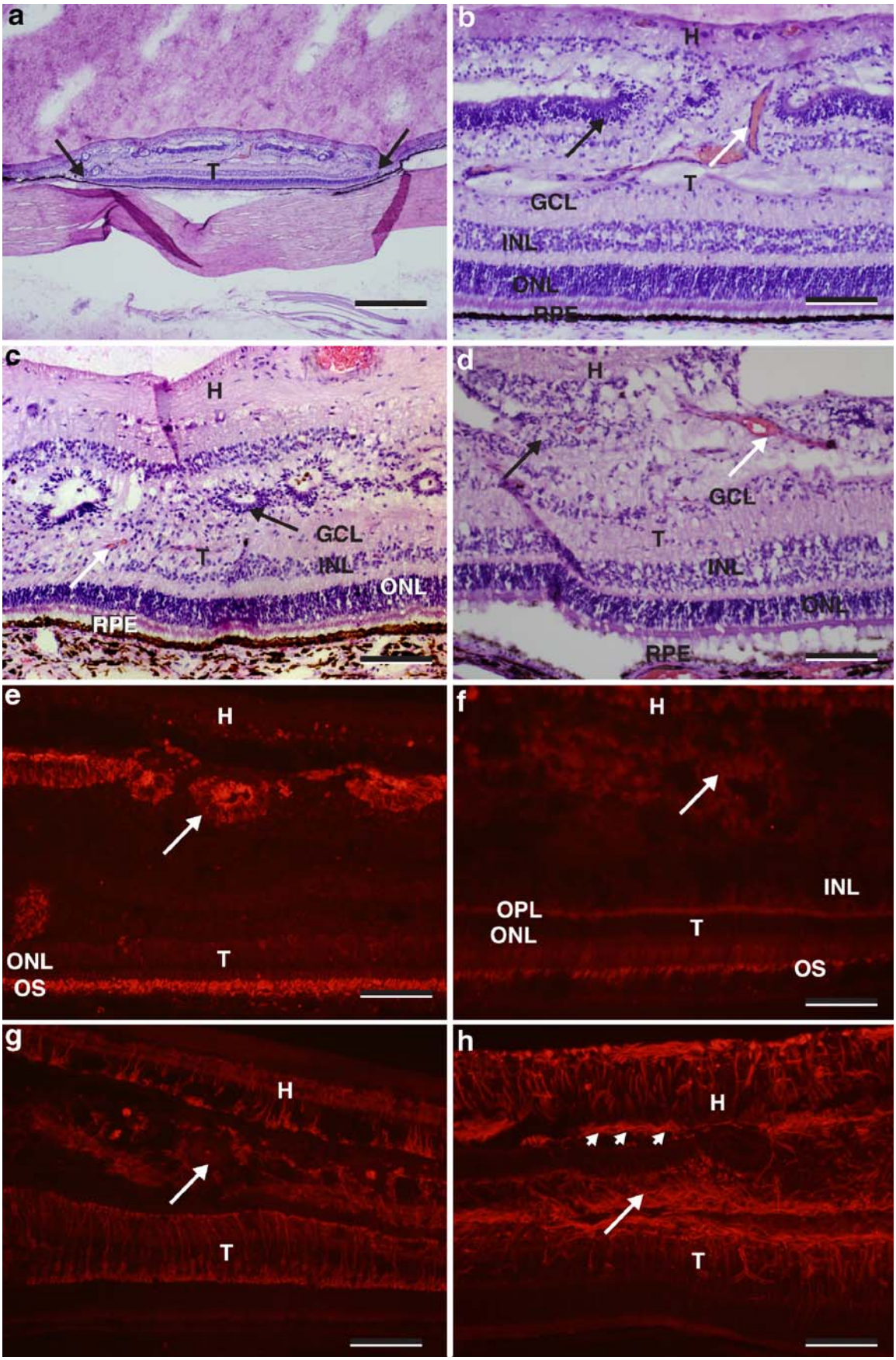
a
T
b
H
GCL
T
INL
ONL
RPE
c
H
GCL
T
INL
ONL
RPE
d
H
GCL
T
INL
ONL
RPE
e
H
T
ONL
OS
f
H
INL
OPL
ONL
T
OS
g
H
T
h
H
T

◀ **Fig. 4** Fetal E48 transplants (*T*) 6 months postop. **a**–**d** Hematoxylin and eosin staining. **e**–**h** Immunohistochemistry. The donor tissue in **a**–**c**, **e**, and **h** was harvested the same day as the operation, while in **d**, **f**, and **g** it was cultured 24–28 h before transplantation. **a**–**d** In **a**, the full extent of the subretinal transplant can be seen (between *arrows*). The transplant measures 2.2 mm. **b**–**d** Details of three different grafts: the transplants (*T*) display a well-laminated part facing the host retinal pigment epithelium (*RPE*) and a more disorganized part facing the remaining host (*H*) neuroretina (*black arrow*). In **c** and **d**, the disorganized part is less pronounced, and some fusion of host and graft retinal layers is present. In **b** and **c**, transplanted photoreceptors in the outer nuclear layer (*ONL*) display a normal organization with short outer segments apposed to a continuous host *RPE*, while the specimen in **d** does not contain as many outer segments and displays a discontinuous host *RPE*. Inner layers of the grafts (*INL* and *GCL*) are well developed. Blood vessels within the grafts are present (*white arrow*). **e** Rhodopsin labeling. The laminated part of the transplant (*T*) displays a normal rhodopsin labeling pattern with labeling concentrated to the outer segment region (*OS*). In the more disorganized part of the graft, labeling is present throughout the rod photoreceptors (*arrow*). A few scattered cells are labeled in the host (*H*) retina. **f** Transducin labeling. The laminated part of the transplant (*T*) displays a normal transducin labeling pattern with labeling concentrated to the cone outer segment region (*OS*). Cone cell bodies in the *ONL*, cone terminals in the *OPL*, and cone bipolar cells in the *IPL* are weakly labeled. Weak and diffuse labeling is seen in the disorganized part of the transplant (*arrow*), and some scattered cells in the host (*H*) display weak labeling. **g** PKC labeling. The laminated part of the transplant (*T*) displays well-labeled and organized rod bipolar cells. In the non-laminated part, well-labeled but disorganized rod bipolar cells are seen (*arrow*). Well-labeled and organized rod bipolar cells are present in the host (*H*) retina, but the density of cells is less than in the normal retina. **h** GFAP labeling. In the laminated part of the transplant (*T*), vertically organized Müller cells can be seen. In the innermost part, labeling is more intense, and labeled structures are horizontally arranged. In the area between the laminated graft and host retina, labeled cells are less organized (*white arrow*). The host retina (*H*) shows normally arranged Müller cells, but gliosis is evident in the outermost part (*arrowheads*). Scale bar=500 μm (**a**), 100 μm (**b**–**e**, **g**, and **h**), 50 μm (**f**)

layers were present but not fully developed. Blood vessels were observed in all grafts either in the disorganized part (Fig. 4b and d) or in the inner layers of the laminated part (Fig. 4c). In one eye no graft could be found (pig #4). In this eye, the retinotomies could be identified, surrounded by an area of host retina without ONL. No signs of inflammation or fibrosis were seen.

Host

The host retina outside the graft area displayed the same appearance in hematoxylin and eosin-stained sections as unoperated control eyes. In the central retina, the ONL displayed 1–3 rows of cells, often with long cone outer segments, the inner retina appeared intact, and the RPE was continuous. The peripheral retina was comparatively thin, in most cases displaying only 1 row of cells in the ONL without outer segments, degenerated inner layers, and a discontinuous RPE. In the host retina straddling the transplant, the ONL was absent except for in a few sections where 1 row of cells with some inner segments remained. The inner layers of the host retina in the transplant area appeared intact in one eye whereas they in the remaining four were thinner than normal. The host RPE facing the transplanted photoreceptors was continuous and well pigmented in four of five eyes (Fig. 4b and c).

Graft-host integration

Due to the presence of non-laminated transplant retina between laminated parts of the host and graft, fusion of the two entities was rarely seen. In two specimens limited areas of fusion of the innermost parts of the graft with the host retina were observed (Fig. 4c and d).

Immunohistochemistry

Rhodopsin

Laminated areas of the transplants displayed a normal expression of rhodopsin, with labeling concentrated to outer segments (Fig. 4e). In rosetted parts of the grafts, labeling was more evenly distributed throughout the rod photoreceptors.

In the host retina straddling the graft, three of the five eyes containing transplants displayed only scattered labeled cells (Fig. 4e). The remaining two host retinas in this area contained 1 and 2 continuous row of cells, respectively. In the host retina outside the transplant area, the five eyes containing transplants displayed 2 rows of rhodopsin-labeled cells in their central part in two cases (Fig. 5a), 1 row in two cases, and scattered cells in one case. In the periphery, one of these five eyes displayed 2 rows of cells, two displayed 1 row of cells (Fig. 5b), and the remaining two only scattered cells. When cell counts of operated eyes were compared with unoperated ones, the five eyes containing transplants displayed significantly more rhodopsin-labeled cells than unoperated controls (Fig. 5a–d, Table 1). The rescue effect of rods was not pronounced in the area adjacent to the transplant but rather in the retina located opposite the location of the graft. The one eye with no graft (pig #4) displayed only scattered rhodopsin-labeled cells throughout the retina (Fig. 5e and f).

Transducin

In the normal adult control retina, the transducin antibody labeled 1–2 rows of cells in the outermost part of the ONL corresponding to cone photoreceptors. Labeling intensity was highest in the outer segments, but cell bodies and terminals in the OPL were also labeled. Weak labeling of cone bipolar cells was also seen. In the laminated part of the transplants, well-labeled cone photoreceptors with a

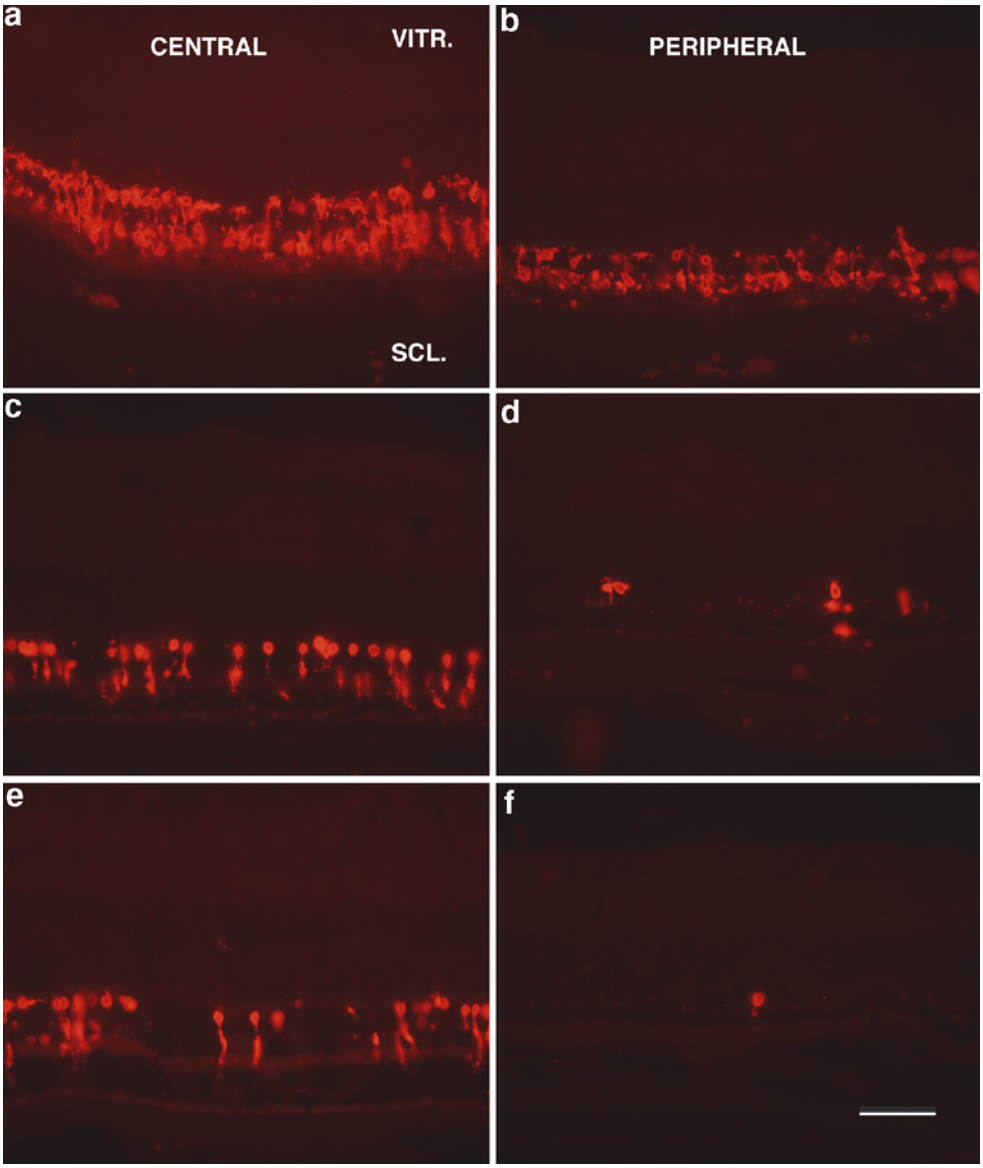

Fig. 5 Rhodopsin labeling of the host retina outside the transplant area. All sections are oriented the same way as in previous figures, i.e., with the vitreal side (*VITR.*) upwards and the scleral (*SCL.*) downwards. **a**, **b** Central and peripheral retina in one of the five operated eyes (pig #1) in which a well-laminated graft was found. **c**, **d** Corresponding retinal regions from the unoperated control eye. **e**, **f** Central and peripheral retina in the operated eye in which no graft was found (pig #4). The host retina in the eye containing a transplant (**a**, **b**) displays significantly more rhodopsin-labeled cells when compared with the unoperated control eye (**c**, **d**) and the operated eye where no transplant was found (**c**, **d**). Scale bar=50 μm

morphology and density comparable to the normal retina were found (Fig. 4f). Some bipolar cells in the inner nuclear layer were weakly labeled. There was no evidence of axonal sprouting of cones or bipolar cells from the graft towards the host. In non-laminated parts of the graft, very weak and diffuse labeling of disorganized structures was found.

In the host retina straddling the graft, scattered labeled cells were observed. In all other areas of the host retina, cone morphology and density of the host retina were comparable to unoperated eyes, revealing 1–2 rows of labeled cells with short axons.

Table 1 Comparison of rhodopsin labeling cell count values (mean± SD) in the host retina in operated (OD) and unoperated (OS) eyes (range in parentheses)

	OD	OS	*p* value
All	42.8±25.9 (12–84)	33.5±18.3 (18.5–66.0)	0.16
All-#4	49.0±23.6 (26.5–84.0)	27.0±10.1 (18.5–42.5)	0.031

Transplants were found in all animals except in #4, and a separate evaluation of the five eyes containing grafts is therefore made in the second row. The Wilcoxon matched pairs signed ranks test was used for statistical comparison.

PKC

In laminated parts of all transplants, well-labeled rod bipolar cells with a normal morphology were seen (Fig. 4g). Non-laminated parts of the grafts often displayed an array of disorganized PKC-labeled cells. No evidence of sprouting rod bipolar axons from the graft towards the host was found. In the host retina, well-labeled and organized rod bipolar cells with axonal processes ending in the host

inner plexiform layer were found. This was also the case in the part straddling the graft, but the density of labeled cells was lower in this area (Fig. 4g). There was no apparent sprouting of rod bipolar dendrites from host to graft.

GFAP

In sections from normal adult porcine eyes, the GFAP antibody labeled horizontally arranged processes in the nerve fiber layer. Weak labeling of vertical Müller cells was also observed throughout the retina. In transplanted as well as in the unoperated eyes, Müller cells throughout the retina were intensely labeled. In the transplants, laminated areas displayed vertically arranged Müller cells throughout the retinal layers with an array of horizontally arranged labeled processes in the innermost part (Fig. 4h). Rosetted and disorganized areas also displayed intense labeling. In the host retina straddling the graft, intensely labeled, vertically arranged Müller cells were seen. In the outermost part, stretches of intensely labeled horizontally arranged structures facing the disorganized part of the graft were seen.

ERG

Table 2 details the results of the ERG measurements. To summarize, b-wave amplitudes of operated eyes increased significantly from 4 to 6 months in the +5 dB but not the −20 dB stimulus group, whereas amplitudes of control eyes decreased significantly in the −20 dB, but not the +5 dB stimulus group (Table 2, left panel).

B-wave amplitudes derived from −20 dB as well as +5 dB stimuli were lower in operated compared with unoperated control eyes in five of six animals at 4 months, but the difference was not significant (Table 2, right side). At 6 months, four of the operated eyes displayed higher b-wave amplitudes than unoperated controls at −20 dB, but again the difference was not statistically different.

Discussion

Transplant survival and development

With this study we have shown that transplantation of fetal full-thickness neuroretina to eyes with severe retinal degeneration is possible and that the grafts survive and develop in the foreign diseased host environment without signs of rejection. In one eye, transplanted with a retina cultured for 24 h, no graft could be found at dissection even though it had been identified in the subretinal space 1 day after surgery. No signs of inflammation macro- or microscopically was seen in the eye, and the most probable reason for the disappearance of the graft is that it escaped through the larger retinotomy and into the vitreous during the postoperative period. The remaining grafts derived from donor tissue kept in culture did not develop differently from donor tissue harvested the same day as the transplantation, which is a very important finding, especially since other neuronal transplantation studies have shown that a substantial amount of donor cells die before actual transplantation [8]. We have previously shown that fetal porcine neuroretina can be kept in culture for extended time periods [9], and we now conclude that cultured tissue can also survive a transplantation procedure.

Cone and rod photoreceptors in the grafts displayed short outer segments, but in other respects developed normally and appeared to integrate well with the host retinal pigment epithelium (RPE). Additionally, most of the inner retinal layers were seen in the grafts which was somewhat surprising. We previously reported that neonatal full-thickness grafts to normal and degenerating hosts do not develop inner layers [15, 16], a phenomenon best explained by the separation from its retinal blood supply [18]. The blood vessels found in all grafts in the present study indicate that fetal full-thickness grafts can develop a new inherent retinal circulation and thereby also form inner layers.

Table 2 Summary of ERG b-wave amplitudes (μV, mean±SD) at 4 and 6 months postoperatively (range in parentheses)

Stimulus	4 months	6 months	*p* value	OD	OS	*p* value
	OD			4 months		
−20 dB	27.7±13.6 (16.6–52.2)	32.1±24.2 (12.5–77.5)	0.500	27.7±13.6 (16.6–52.2)	49.1±19.0 (24.7–74.3)	0.11
+5 dB	130.5±66.1 (61.9–209.1)	181.4±76.1 (85.6–269.1)	0.047	130.5±66.1 (61.9–209.1)	209.2±47.4 (24.7–74.3)	0.078
	OS			6 months		
−20 dB	49.1±19.0 (24.7–74.3)	24.2±13.2 (8.3–41.3)	0.031	32.1±24.2 (12.5–77.5)	24.2±13.2 (8.3–41.3)	0.34
+5 dB	209.2±47.4 (24.7–74.3)	197.8±56 (148.4–291.9)	0.34	181.4±76.1 (85.6–269.1)	197.8±56 (148.4–291.9)	0.28

Amplitudes derived from −20 dB and +5 dB stimulus intensity are given. *OD* operated eye (oculus dexter), *OS* unoperated control eye (oculus sinister). On the left side of the table, operated and unoperated eyes are evaluated separately, and on the right side, operated and unoperated eyes are compared at each time point. The Wilcoxon matched pairs signed ranks test was used for statistical comparison.

Graft-host integration

In routine stained sections, graft and host retina appeared to fuse occasionally, but a more detailed analysis showed that the two entities did not form neuronal connections. The lack of neuronal integration can be ascribed to several factors. First, physical barriers between laminated parts of the graft and host retina exist in the form of horizontally arranged GFAP-expressing fibers in the innermost part of the graft as well as the outermost part of the host retina. In the host retina this is best explained by Müller cell hypertrophy and proliferation induced by the detachment from the normal choroidal support, as well as the inherent retinal degenerative disease [10, 20]. In the graft, the horizontal inner retinal structures most probably do not represent gliosis, but rather normal processes derived from astrocytes and Müller cells which are found in abundance in the normal porcine retina [19]. We have not seen such fibers in grafts derived from neonatal donor tissue, and the present finding again demonstrates a difference in inner retinal development between fetal and neonatal porcine transplants. Second, another physical barrier is present in the form of non-laminated transplant retina between laminated parts of the host and graft. This phenomenon, indicating abnormal growth of the graft along the scleral-vitreal axis, has not been found in eyes transplanted with neonatal or adult donor tissue [16, 31], but has been noted in short-term fetal rabbit grafts [11]. Evidently, the confined space in the subretinal space does not allow lateral expansion of the graft, which would be more desirable. As a consequence, the grafts become double-folded where the part facing the host RPE develops normally and the one facing the host neuroretina degenerates. The third factor preventing neuronal integration is the lack of sprouting fibers from transplanted photoreceptors as well as host- and graft-derived rod bipolar cells. In previous work, we have seen that fetal rabbit full-thickness grafts initially develop all retinal layers, including ganglion cells [14], but that inner retinal layers after 6–10 months dissolve and start to sprout rod bipolar fibers towards the host [12]. In the present study, inner retinal layers of the grafts appeared to be more preserved compared with long-term fetal rabbit grafts. This difference may be explained by the completely vascularized nature of the porcine retina in contrast to the merangiotic nature of the rabbit retina [7]. Whether it is possible to induce sprouting in a completely vascularized retina without sacrificing the intricate organization of retinal neurons is indeed a great future challenge for retinal transplantation research.

Host retina

Earlier investigations of the rhodopsin transgenic pig have shown that the ERG rod response to blue light stimulus is severely reduced already at 4 weeks of age [25]. Using a different ERG protocol involving white light flashes, we found that the rhodopsin transgenic eyes responded to a wide range of stimulus intensities enabling monitoring of both rod and cone function. One of the transplanted eyes (pig #1) developed a cataract which prevented proper visualization of the fundus and ERG recording, but in the remaining 11 eyes (5 operated and 6 unoperated controls), the −20 dB response obtained at 6 months postoperatively corresponded well to the number of remaining rods found using rhodopsin immunohistochemistry (individual data not shown).

At 4 months postoperatively, we found that both rod and cone responses in operated eyes were lower than in the unoperated controls in the majority of cases. Although this difference did not quite reach statistical significance, the finding indicates that host retinal function, at least temporarily, is reduced by the surgical procedure involved in the transplantation. Several steps in the transplantation protocol need to be considered when evaluating any adverse effect on the host retina. Access to the subretinal space can be gained by an external route passing through the sclera, choroid, Bruch's membrane, and RPE. This approach is commonly used in experiments involving small animals with a comparatively large lens [32]. Subretinal surgery in larger animal or human eyes is invariably performed by an intravitreal approach which enables full visual inspection of the surgical area and additionally minimizes the risk of choroidal hemorrhage and disruption of the outer blood-retina barrier. However, vitrectomy and the formation of a localized retinal detachment are potentially harmful components of the surgery, which may help to explain the initial loss of retinal function compared with unoperated eyes [5, 33]. Also, the recent discovery that modest amounts of light may permanently damage the RP retina is of interest in the vitrectomy setting, since a relatively bright intraocular illuminator is used close to the retina [4]. In eyes containing transplants, however, b-wave amplitudes increased significantly from 4 to 6 months, indicating that the traumatic effect of the surgery can be counteracted by the presence of a well-developed graft. Photoreceptors and bipolar cells in the laminated graft could theoretically contribute to the ERG response, but the comparatively small transplant area makes this unlikely. A more plausible theory for the increased response at 6 months is that the initial traumatic effect of the surgery is counteracted by the presence of a surviving graft. Host cone rescue after transplantation has been previously observed and has been ascribed to the presence of a cone survival factor in the transplanted rods [1, 24]. The significantly higher number of rod photoreceptors in eyes with transplants compared with unoperated control eyes provides further proof that normal neuroretinal tissue can influence the

degenerating retina favorably. We did not include sham-operated control eyes in our study, which would have been very useful when evaluating the rescuing effect of the surviving graft. However, the transplanted eye without a graft displayed almost no surviving rods, implying a traumatic long-term effect from the surgery which was not compensated by trophic support from a surviving graft.

Interestingly, host rod survival in eyes containing transplants was more pronounced at some distance from the graft, indicating that the rod rescuing effect is not a local phenomenon. Possible candidates responsible for the host rod rescue include growth factors as well as several other substances expressed in the normal neuroretina [23].

Conclusion

Fetal full-thickness neuroretina can safely be transplanted to a human-sized eye with a severe retinal degeneration. In their major part, the transplants develop a normal laminated morphology and survive for at least 6 months without signs of graft rejection. Short-term culturing of the donor tissue preoperatively does not seem to adversely influence graft survival. Host and graft retinal neurons do not form connections due to the presence of disorganized graft tissue, gliotic changes in the host retina, and lack of sprouting retinal neurons. Rod survival and retinal function in the host are affected unfavorably by the surgical trauma, but the presence of a well-laminated graft counteracts this effect and can rescue rods from degeneration. Retinal transplantation has mainly been aimed at replacing diseased photoreceptors, but the prospect of rescuing such cells by trophic support from a surviving retinal graft may open new avenues in the treatment of RP.

Acknowledgements The authors extend their gratitude to Karin Arnér, Jill Barnes, Bruce Collins, Donna Hardin and Jeff Sommer.

References

1. Arai S, Thomas BB, Seiler MJ, Aramant RB, Qiu G, Mui C, de Juan E, Sadda SR (2004) Restoration of visual responses following transplantation of intact retinal sheets in rd mice. Exp Eye Res 79:331–341
2. Berson EL, Rosner B, Sandberg MA, Weigel-DiFranco C, Dryja TP (1991) Ocular findings in patients with autosomal dominant retinitis pigmentosa and rhodopsin, proline-347-leucine. Am J Ophthalmol 15:614–623
3. Brundin P, Karlsson J, Emgard M, Schierle GS, Hansson O, Petersen A, Castilho RF (2000) Improving the survival of grafted dopaminergic neurons: a review over current approaches. Cell Transplant 9:179–195
4. Cideciyan AV, Jacobson SG, Aleman TS, Gu D, Pearce-Kelling SE, Sumaroka A, Acland GM, Aguirre GD (2005) In vivo dynamics of retinal injury and repair in the rhodopsin mutant dog model of human retinitis pigmentosa. Proc Natl Acad Sci USA 102:5233–5238
5. Cook B, Lewis GP, Fisher SK, Adler R (1995) Apoptotic photoreceptor degeneration in experimental retinal detachment. Invest Ophthalmol Vis Sci 36:990–996
6. Das T, del Cerro M, Jalali S, Rao VS, Gullapalli VK, Little C, Loreto DA, Sharma S, Sreedharan A, del Cerro C, Rao GN (1999) The transplantation of human fetal neuroretinal cells in advanced retinitis pigmentosa patients: results of a long-term safety study. Exp Neurol 157:58–68
7. De Schaepdrijver L, Simoens P, Lauwers H, De Geest JP (1989) Retinal vascular patterns in domestic animals. Res Vet Sci 47:34–42
8. Emgard M, Blomgren K, Brundin P (2002) Characterisation of cell damage and death in embryonic mesencephalic tissue: a study on ultrastructure, vital stains and protease activity. Neuroscience 115:1177–1187
9. Engelsberg K, Johansson K, Ghosh F (2005) Development of the embryonic porcine neuroretina in vitro. Ophthalmic Res 37:104–111
10. Fisher SK, Lewis GP (2003) Müller cell and neuronal remodeling in retinal detachment and reattachment and their potential consequences for visual recovery: a review and reconsideration of recent data. Vision Res 43:887–897
11. Ghosh F, Arnér K, Ehinger B (1998) Transplant of full-thickness embryonic rabbit retina using pars plana vitrectomy. Retina 18:136–142
12. Ghosh F, Bruun A, Ehinger B (1999) Graft-host connections in long-term full thickness embryonic rabbit retinal transplants. Invest Ophthalmol Vis Sci 40:126–132
13. Ghosh F, Johansson K, Ehinger B (1999) Long-term full-thickness embryonic rabbit retinal transplants. Invest Ophthalmol Vis Sci 40:133–140
14. Ghosh F, Bruun A, Ehinger B (1999) Immunohistochemical markers in well laminated retinal transplants. Ophthalmic Res 31:5–15
15. Ghosh F, Arnér K (2002) Transplantation of full-thickness retina in the normal porcine eye-surgical and morphological aspects. Retina 22:478–486
16. Ghosh F, Wong F, Johansson K, Bruun A, Petters RM (2004) Transplantation of full-thickness retina in the rhodopsin transgenic pig. Retina 24:98–109
17. Gouras P, Du J, Kjeldbye H, Yamamamoto S, Zack DJ (1994) Long-term photoreceptor transplants in dystrophic and normal mouse retina. Invest Ophthalmol Vis Sci 35:3145–3153
18. Hayreh SS, Kolder HE, Weingeist TA (1980) Central retinal artery occlusion and retinal tolerance time. Ophthalmology 87:75–78
19. Jackson TL, Hillenkamp J, Williamson TH, Clarke KW, Almubarak AI, Marshall J (2003) An experimental model of rhegmatogenous retinal detachment: surgical results and glial cell response. Invest Ophthalmol Vis Sci 44:4026–4034
20. Jones BW, Watt CB, Frederick JM, Baehr W, Chen CK, Levine EM, Milam AH, Lavail MM, Marc RE (2003) Retinal remodeling triggered by photoreceptor degenerations. J Comp Neurol 464:1–16
21. Kwan AS, Wang S, Lund RD (1999) Photoreceptor layer reconstruction in a rodent model of retinal degeneration. Exp Neurol 159:21–33
22. Li ZY, Wong F, Chang JH, Possin DE, Hao Y, Petters RM, Milam AH (1998) Rhodopsin transgenic pigs as a model for human retinitis pigmentosa. Invest Ophthalmol Vis Sci 39:808–819
23. Lund RD, Kwan AS, Keegan DJ, Sauve Y, Coffey PJ, Lawrence JM (2001) Cell transplantation as a treatment for retinal disease. Prog Retin Eye Res 20:415–449
24. Mohand-Said S, Hicks D, Dreyfus H, Sahel JA (2000) Selective transplantation of rods delays cone loss in a retinitis pigmentosa model. Arch Ophthalmol 118:807–811
25. Petters RM, Alexander CA, Wells KD, Collins EB, Sommer JR, Blanton MR, Rojas G, Hao Y, Flowers WL, Banin E, Cideciyan

AV, Jacobson SG, Wong F (1997) Genetically engineered large animal model for studying cone photoreceptor survival and degeneration in retinitis pigmentosa. Nat Biotechnol 15:965–970
26. Radner W, Sadda SR, Humayun MS, Suzuki S, Melia M, Weiland J, de Juan E Jr (2001) Light-driven retinal ganglion cell responses in blind rd mice after neural retinal transplantation. Invest Ophthalmol Vis Sci 42:1057–1065
27. Radtke ND, Aramant RB, Seiler MJ, Petry HM, Pidwell D (2004) Vision change after sheet transplant of fetal retina with retinal pigment epithelium to a patient with retinitis pigmentosa. Arch Ophthalmol 122:1159–1165
28. Seiler MJ, Sagdullaev BT, Woch G, Thomas BB, Aramant RB (2005) Transsynaptic virus tracing from host brain to subretinal transplants. Eur J Neurosci 21:161–172
29. Sharma RK, Bergstrom A, Zucker CL, Adolph AR, Ehinger B (2000) Survival of long-term retinal cell transplants. Acta Ophthalmol 78:396–402
30. Turner JE, Blair JR (1986) Newborn rat retinal cells transplanted into a retinal lesion site in adult host eyes. Brain Res 391:91–104
31. Wassélius J, Ghosh F (2001) Adult rabbit retinal transplants. Invest Ophthalmol Vis Sci 42:2632–2638
32. Woch G, Aramant RB, Seiler MJ, Sagdullaev BT, McCall MA (2001) Retinal transplants restore visually evoked responses in rats with photoreceptor degeneration. Invest Ophthalmol Vis Sci 42:1669–1676
33. Yoshida A, Ishiguro S, Tamai M (1993) Expression of glial fibrillary acidic protein in rabbit Muller cells after lensectomy-vitrectomy. Invest Ophthalmol Vis Sci 34:3154–3160